

# FINAL RESULTS ON HEAVY QUARKS AT LEP AND SLD

Achille Stocchi

Laboratoire de l'Accélérateur Linéaire,  
IN2P3-CNRS et Université de Paris-Sud, BP34, F-91898 Orsay Cedex, France.

## ABSTRACT

In the last decade, the LEP and SLD experiments played a central role in the study of B hadrons (hadrons containing a  $b$  quark). New B hadrons have been observed ( $B_s^0$ ,  $\Lambda_b$ ,  $\Xi_b$  and  $B^{**}$ ) and their production and decay properties have been measured. In this paper we will focus on measurements of the CKM matrix elements:  $|V_{cb}|$ ,  $|V_{ub}|$ ,  $|V_{td}|$  and  $|V_{ts}|$ . We will show how all these measurements, together with theoretical developments, have significantly improved our knowledge on the flavour sector of the Standard Model.

# 1 Introduction

B physics studies are exploiting a unique laboratory for testing the Standard Model in the fermion sector, for studying the QCD in the non-perturbative regime and for searching for New Physics through virtual processes.

In the last decade, the LEP and SLD experiments played an important role in the study of B hadrons. At the start of the LEP and SLC accelerator in 1989, only the  $B_d$  and the  $B^+$  hadrons were known and their properties were under study. New weakly decaying B hadrons have been observed ( $B_s^0$ ,  $\Lambda_b$ ,  $\Xi_b$ ) for the first time and their production and decay properties have been measured. New strongly decaying hadrons, the orbitally (L=1) excited B ( $B^{**}$ ) mesons have been also observed and their mass and production rates measured.

In this paper we will focus on the measurements of the CKM matrix elements :  $V_{cb}$  and  $V_{ub}$  through B decays and  $V_{td}$  and  $V_{ts}$  using  $B^0 - \bar{B}^0$  oscillations. On the other hand many additional measurements on B meson properties (mass, branching fractions, lifetimes...) are necessary to constrain the Heavy Quark theories (Operator Product Expansion (OPE) /Heavy Quark Effective Theory (HQET) /Lattice QCD (LQCD)) to allow for precise extraction of the CKM parameters. We finally show how these measurements constrain the Standard Model in the fermion sector, through the determination of the unitarity triangle parameters.

In this paper we try to compare the LEP/SLD results with those obtained from other collaborations (CLEO at Cornell, CDF at TeVatron and the asymmetric B-factories: BaBar and Belle) and to present, when available, the world average result. A detailed description of the results and of the averaging techniques can be found in.<sup>1,2</sup>

## 2 B physics at the $Z^0$

At the  $Z^0$  resonance, B hadrons are produced from the coupling of the  $Z^0$  to a  $b\bar{b}$  quark pair. The production cross section is of  $\sim 6$  nb, which is five times larger than at the  $\Upsilon(4S)$ . Because of the specific (V-A) behaviour of the electroweak coupling at the  $Z^0$  pole, hadronic events account for about 70% of the total production rate; among these, the fraction of  $b\bar{b}$  events is  $\sim 22\%$ . Because of the energy available only  $B^+$  and  $B_d^0$  mesons can be produced at the  $\Upsilon(4S)$ . The

B particles are produced almost at rest (the average momentum is of about 350 MeV/c), with no accompanying additional hadrons, and the decay products of the two B particles are spread isotropically over the space. At the Z pole, the primary  $b\bar{b}$  pair, picks up from the vacuum other quark-antiquarks pairs and hadronizes into B hadrons plus few other particles. Therefore not only  $B^\pm$  and  $B_d$  mesons are produced, but also  $B_s^0$  mesons or B baryons can be present in the final state. The  $b$  and the  $\bar{b}$  hadronize almost independently.  $b$  quarks fragment differently from light quarks, because of their high mass as compared with  $\Lambda_{QCD}$ . B hadrons carry, on average, about 70% of the available beam energy, whereas the rest of the energy is distributed among the other fragmenting particles. As a consequence, the two B hadrons fly in opposite directions and their decay products form jets situated in two opposite hemispheres.

The hard fragmentation and the long lifetime of the b quark make that the flight distance of a B hadron at the Z pole, defined as  $L = \gamma\beta c\tau$ , on average of the order of 3 mm. As decay products have a mean charged multiplicity of 5<sup>\*</sup>, it was possible to tag B hadrons using a lifetime tag.

Most of the precision measurements in B physics performed at LEP/SLC, Tevatron and B factories, would not have been possible without the development of Silicon micro vertex detectors. In practice the averaged flight distance of the B hadrons becomes measurable thanks to the precision of silicon detectors, located as close as possible to the beam interaction point. These detectors determine with a precision better than 10  $\mu m$ , the position of a charged particle trajectory. In particular the separation between  $b$  quarks and other quarks is mainly based on the use of vertex detectors. Charged particles produced at the B vertex (secondary vertex) can be separated from those produced at the interaction point (primary vertex) using the precise tracking information. In spite of the relatively small statistics collected by the SLD experiment, it gave very important and competitive contributions to B physics, because of its silicon vertex detectors, which is located very close to the interaction point. A typical LEP  $b\bar{b}$  event is shown in Figure 1.

Because of the large B mass, B hadrons are expected to decay into several decay modes with branching ratio of the order of a per mille. According to the registered statistics, at LEP, inclusive or semi-exclusive  $b$ -hadron decays had to be

---

\*On average there are as many particles originating from  $b$ -quark fragmentation and from B decay.

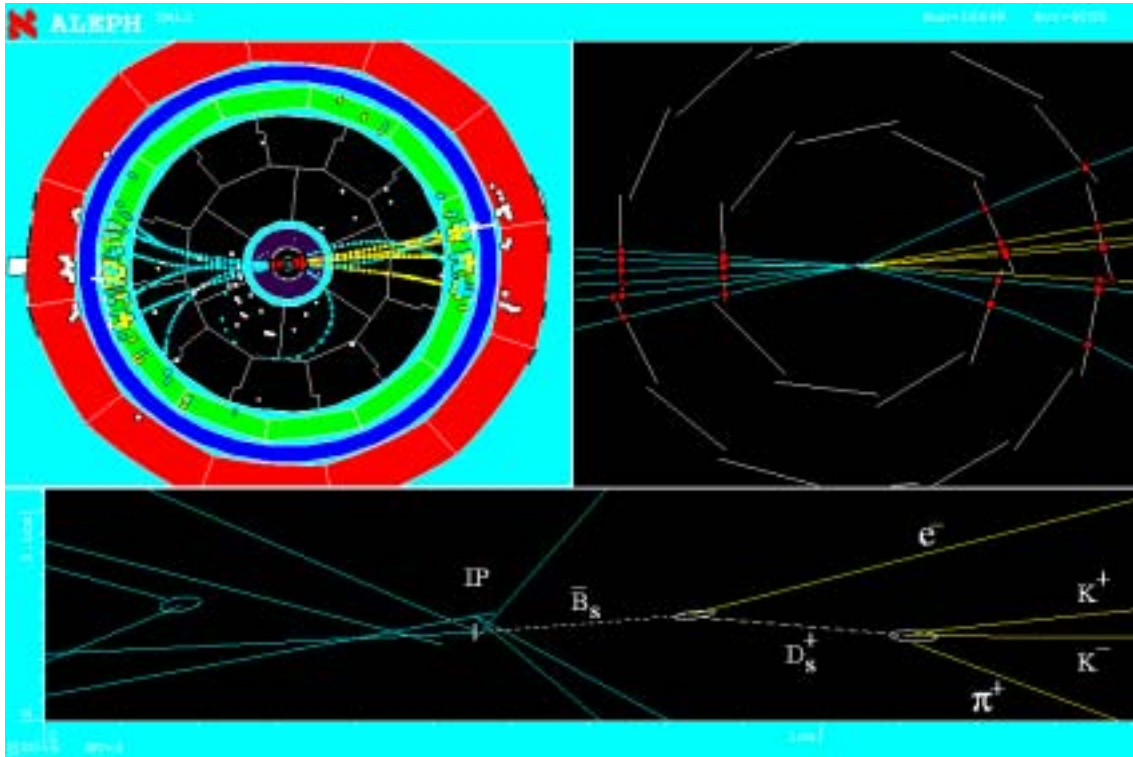


Figure 1: A  $LEP\ b\bar{b}$  event. In the upper part, the ALEPH detector and a zoom on the charged tracks seen by the silicon detectors are displayed. In the lower part the reconstructed event is shown. The event is constituted of two jets which define two separate hemispheres. In one of these hemispheres a  $\bar{B}_s^0$  decays semileptonically :  $\bar{B}_s^0 \rightarrow D_s^+ e^- \bar{\nu}_e X$  (secondary vertex), followed by the decay :  $D_s^+ \rightarrow K^+ K^- \pi^+$  (tertiary vertex). The primary vertex (marked with IP) is also shown.

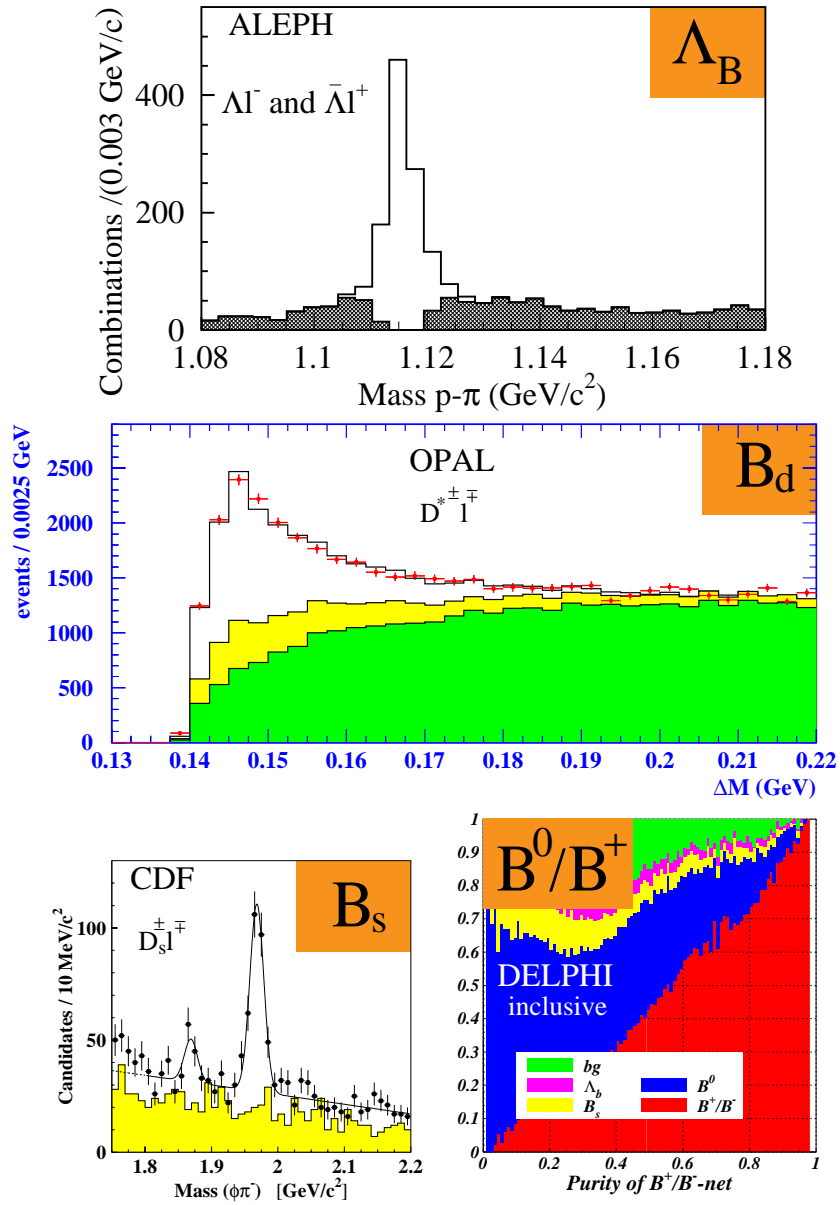


Figure 2: The three plots from top-left to bottom-left show the invariant mass spectra of  $\Lambda$ ,  $((D^0\pi) - D^0)$  and  $D_s$  which are obtained in correlation with an opposite sign lepton. These events are attributed mainly to the semileptonic decays of  $\Lambda_B$ ,  $B_d^0$  and  $B_s^0$  hadrons, respectively. The bottom-right figure shows the possibility of distinguishing the charged and neutral  $B$  mesons based on inclusive techniques.

studied in place of exclusive channels for which very few events are expected<sup>†</sup>. Semileptonic decays benefit of a large branching ratio ( of the order of 10% ) and of clean and easily distinguishable final states. Semileptonic decays allow also to distinguish between different types of  $b$  hadrons, by reconstructing charmed hadrons. As an example, a  $\Lambda_c^+$  accompanied by a lepton with negative electric charge, in a jet, signs a  $b$ -baryon. For baryons, it is not even necessary to completely reconstruct the  $\Lambda_c^+$  charmed baryon, correlations as  $p\ell^-$  or  $\Lambda\ell^-$  are sufficient. Similarly,  $D_s^+\ell^-$  or  $D^*\ell^-$  events in a jet, provide event samples enriched in  $\bar{B}_s^0$  and  $\bar{B}_d^0$  mesons respectively.

An overview of the signals used to study these new states is given in Figure 2.

### 3 Example of historical evolution

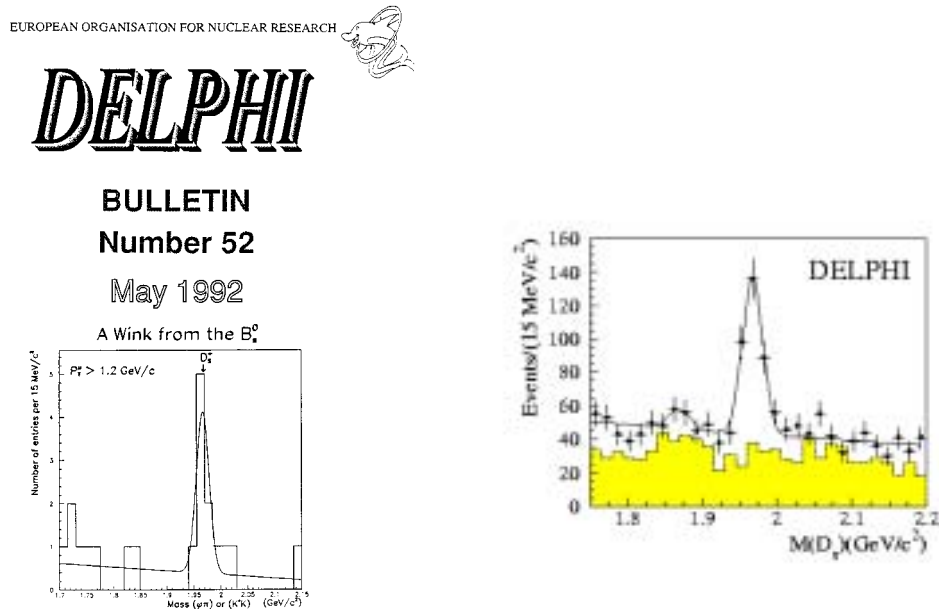


Figure 3: *The left plot shows the first signal of the  $\bar{B}_s^0$  meson in 1992, seen in the semileptonic decay :  $\bar{B}_s^0 \rightarrow D_s^+\ell^-\bar{\nu}_\ell$ , whereas the right plot shows the same signal few years later.*

<sup>†</sup>with the final LEP statistics, B rare decays with branching fraction of the order of a few  $10^{-5}$  could be accessed.

We take the example of the  $B_s^0$  meson to illustrate how our knowledge on the properties of B hadrons has evolved during the last ten years. In 1992, 7 events  $\bar{B}_s^0 \rightarrow D_s^+ \ell^- \bar{\nu}_\ell$ , constituted the first evidence for the  $B_s^0$  meson. A few years later the same signal consists of more than 200 events.

In the mean time our knowledge has much improved: the fraction of  $B_s^0$  mesons in b jets is precisely measured as well as the  $B_s^0$  mass and lifetime.

- the  $\bar{B}_s^0$  rate in  $b$ -jets amounts to:  $f_s = (9.7 \pm 1.2)\%$ ,
- the  $B_s^0$  meson mass is  $m_{B_s^0} = (5369.6 \pm 2.4)MeV$  (CDF mainly)
- the lifetime is  $\tau(\bar{B}_s^0) = 1.464 \pm 0.057 ps$ .
- the studies on  $B_s^0 - \bar{B}_s^0$  oscillations give  $\Delta m_s > 15ps^{-1}$  (95% C.L.)
- the ratio  $\Delta\Gamma_{B_s^0}/\Gamma_{B_s^0} < 0.31$  (95% C.L.)

## 4 Heavy hadron lifetimes

Measurements of B lifetimes test the decay dynamics, giving important information on non-perturbative QCD corrections induced by the spectator quark (or diquark). Decay rates are expressed using the OPE formalism, as a sum of operators developed in series of order  $O(\Lambda_{QCD}/m_Q)^n$ . In this formalism, no term of order  $1/m_Q$  is present and spectator effects contribute at order  $1/m_Q^3$ <sup>‡</sup>. Non-perturbative operators are evaluated, most reliably, using lattice QCD calculations.

### 4.1 Beauty hadron lifetimes

Since the beginning of the LEP/SLD data taking an intense activity has been concentrated on the studies of B hadron lifetimes.

Results are given in Table 1.<sup>3</sup>

Figure 4.1 gives the ratios of different B hadron lifetimes, as compared with theory predictions (dark(yellow) bands).

The achieved experimental precision is remarkable and LEP results are still dominating the scene. The fact that charged B mesons live longer than neutral B

<sup>‡</sup>Terms at order  $1/m_Q$  would appear if in this expansion the mass of the heavy hadron was used instead of the mass of the quark. The presence of such a term would violate the quark-hadron duality.

Table 1: Summary of B hadron lifetime results (as calculated by the Lifetime Working Group<sup>3</sup>).

B Hadrons	Lifetime [ps]	
$\tau(B_d^0)$	$1.540 \pm 0.014$	(0.9 %)
$\tau(B^+)$	$1.656 \pm 0.014$	(0.8 %)
$\tau(B_s^0)$	$1.461 \pm 0.057$	(3.9 %)
$\tau(\Lambda_b^0)$	$1.208 \pm 0.051$	(4.2 %)
$\tau(B_d^0)/\tau(B^+)$	= $1.073 \pm 0.014$	
$\tau(B_d^0)/\tau(B_s^0)$	= $0.949 \pm 0.038$	
$\tau(\Lambda_b^0)/\tau(B_d^0)$	= $0.798 \pm 0.052$	
$\tau(b - \text{bar})/\tau(B_d^0)$	= $0.784 \pm 0.034$	

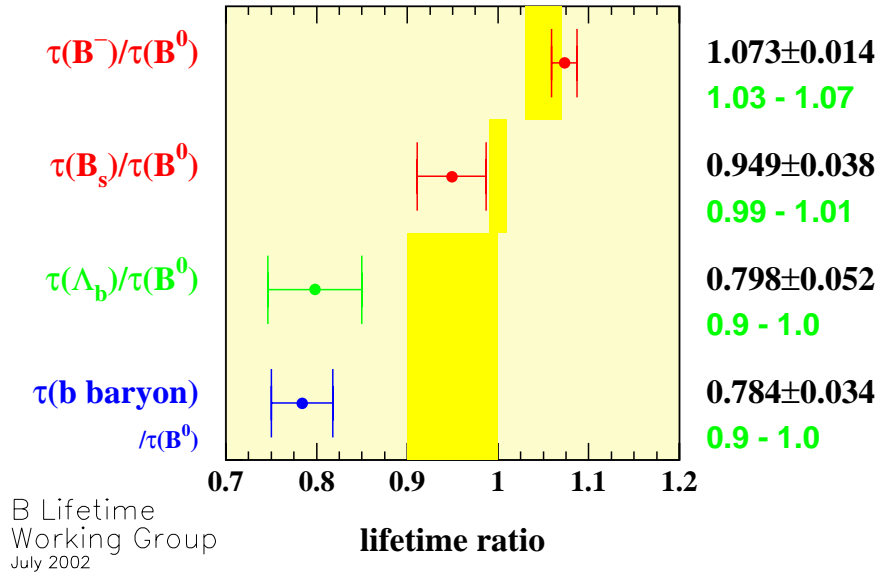


Figure 4: B hadrons lifetime ratios,<sup>3</sup> compared with the theoretical predictions as given by the dark(yellow) bands.

mesons is now established at  $5\sigma$  level and is in agreement with theory. The  $B_d^0$  and  $B_s^0$  lifetimes are expected (at  $\simeq 1\%$ ) and found (at  $\simeq 4\%$ ) to be equal. A significant

measurement in which this ratio differs from unity will have major consequences for the theory. The lifetime of the b-baryons is measured to be shorter than the  $B_d^0$  lifetime, but the size of this effect seems to be more important than predicted ( $2-3\sigma$ ). Recent calculations of high order terms give an evaluation of the b-baryon lifetime in better agreement with the experimental result.<sup>4</sup>

New results are expected from B-Factories (which could decrease the relative error on the lifetimes of the  $B_d^0$  and  $B^+$  to 0.4-0.5%) and mainly from Tevatron (Run II) which could precisely measure all B hadron lifetimes, including those for the  $\Xi_b$ ,  $\Omega_b$  and the  $B_c$ .

In figure 5 the improvement on the precision of the measured B hadron lifetimes over the years is shown.

## 5 Determination of the CKM element: $|V_{cb}|$

The  $|V_{cb}|$  element of the CKM matrix can be accessed by studying the rates of inclusive and exclusive semileptonic  $b$ -decays.

### 5.1 $|V_{cb}|$ inclusive analyses.

The first method to extract  $|V_{cb}|$  makes use of the inclusive semileptonic decays of B-hadrons and of the theoretical calculations done in the framework of the OPE. The inclusive semileptonic width  $\Gamma_{s.l.}$  is expressed as:

$$\Gamma_{s.l.} = \frac{BR(b \rightarrow cl\nu)}{\tau_b} = \gamma_{theory} |V_{cb}|^2;$$

$$\gamma_{theory} = f(\alpha_s, m_b, \mu_\pi^2, 1/m_b^3 \dots). \quad (1)$$

From the experimental point of view the semileptonic width has been measured by the LEP/SLD and  $\Upsilon(4S)$  experiments with a relative precision of about 2%<sup>5</sup>:

$$\begin{aligned} \Gamma_{sl} &= (0.431 \pm 0.008 \pm 0.007) 10^{-10} MeV && \Upsilon(4S) \\ \Gamma_{sl} &= (0.439 \pm 0.010 \pm 0.007) 10^{-10} MeV && \text{LEP/SLD} \\ \Gamma_{sl} &= (0.434 \times (1 \pm 0.018)) 10^{-10} MeV && \text{ave.} \end{aligned} \quad (2)$$

The precision on the determination of  $|V_{cb}|$  is mainly limited by theoretical uncertainties on the parameters entering in the expression of  $\gamma_{theory}$  in equation 1.

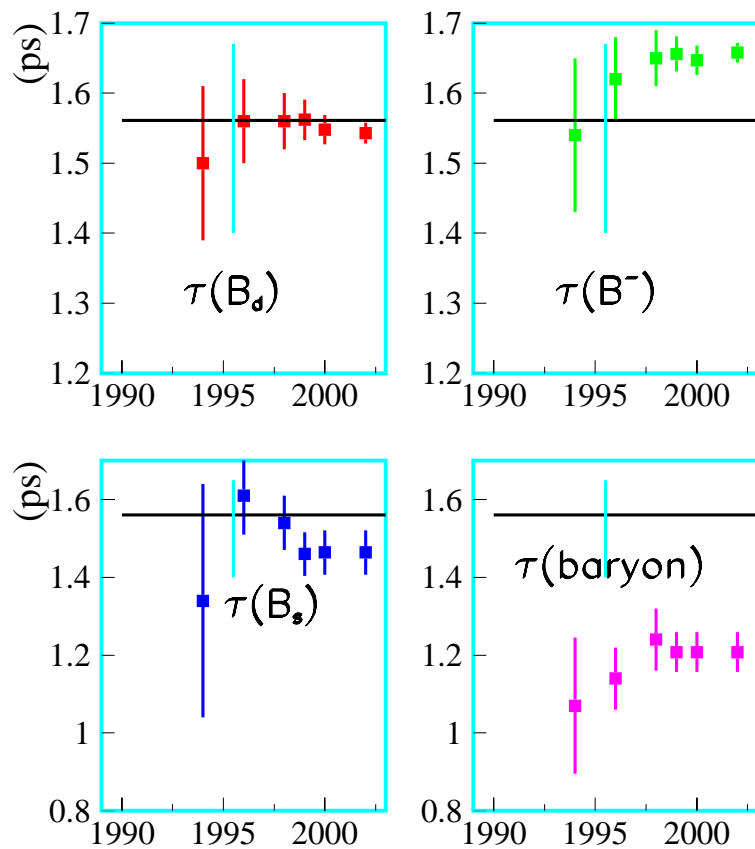


Figure 5: Evolution of the combined measurement of the different B hadron lifetimes over the years. The vertical band, in each plot, indicates the end of the data taking at LEP.

## 5.2 Moments analyses

Moments of the hadronic mass spectrum, of the lepton energy spectrum and of the photon energy in the  $b \rightarrow s\gamma$  decay are sensitive to the non perturbative QCD parameters contained in the factor  $\gamma_{theory}$  of equation 1 and in particular to the mass of the  $b$  and  $c$  quarks and to the Fermi motion of the heavy quark inside the hadron,  $\mu_\pi^2$  <sup>§</sup>.

Results from DELPHI collaboration are shown in Figure 5.2.

Similar results (and with comparable precision) have been obtained by CLEO (which did a pioneering work in this field) and by the BaBar Coll..<sup>2</sup>

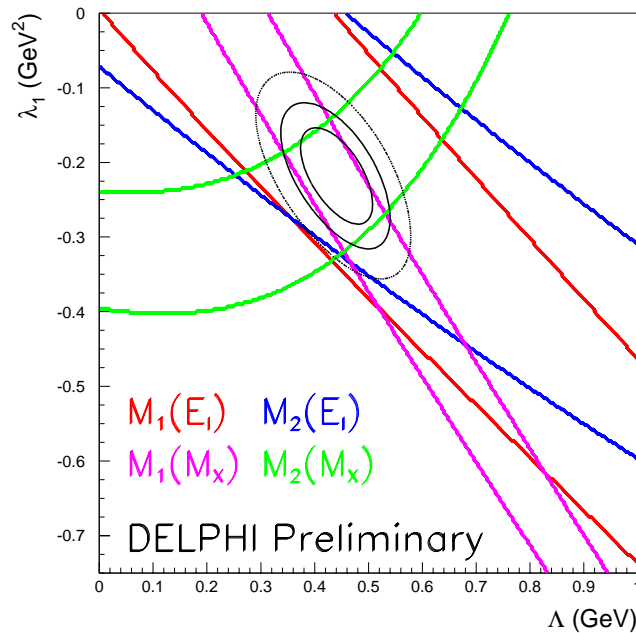


Figure 6: Constraints in the  $\bar{\Lambda} - \lambda_1$  plane obtained: by the DELPHI Coll. using the measured values of the first two moments of the hadronic mass and lepton energy spectra. The bands represent the  $1\sigma$  regions selected by each moment and the ellipses show the 39%, 68% and 90% probability regions of the global fit.

<sup>§</sup>In another formalism, based on pole quark masses, the  $\bar{\Lambda}$  and  $\lambda_1$  parameters are used, which can be related to the difference between hadron and quark masses and to  $\mu_\pi^2$ , respectively.

Using the experimental results on  $\bar{\Lambda}$  and  $\lambda_1$ :

$$|V_{cb}| = (40.7 \pm 0.6 \pm 0.8(\text{theo.}))10^{-3}(\text{inclusive}) \quad (3)$$

This result corresponds to an important improvement on the determination of the  $|V_{cb}|$  element. Part of the theoretical errors (from  $m_b$  and  $\mu_\pi^2$ ) is now absorbed in the experimental error and the theoretical error is reduced by a factor two. The remaining theoretical error could be further reduced if the parameters controlling the  $1/m_b^3$  corrections are extracted directly from experimental data.

### 5.3 $|V_{cb}|$ : $B \rightarrow D^* \ell \nu$ analyses.

An alternative method to determine  $|V_{cb}|$  is based on exclusive  $\overline{B}_d^0 \rightarrow D^{*+} \ell^- \bar{\nu}_\ell$  decays. Using HQET, an expression for the differential decay rate can be derived

$$\frac{d\Gamma}{dw} = \frac{G_F^2}{48\pi^2} |V_{cb}|^2 |F(w)|^2 G(w) ; w = v_B \cdot v_D \quad (4)$$

$w$  is the relative velocity between the B ( $v_B$ ) and the D systems ( $v_D$ ).  $G(w)$  is a kinematical factor and  $F(w)$  is the form factor describing the transition. At zero recoil ( $w=1$ )  $F(1)$  goes to unity. The strategy is then to measure  $d\Gamma/dw$ , to extrapolate at zero recoil and to determine  $F(1) \times |V_{cb}|$ .

The experimental results are summarised in Figure 7. Using  $F(1) = 0.91 \pm 0.04$ ,<sup>6</sup> it gives<sup>5</sup>:

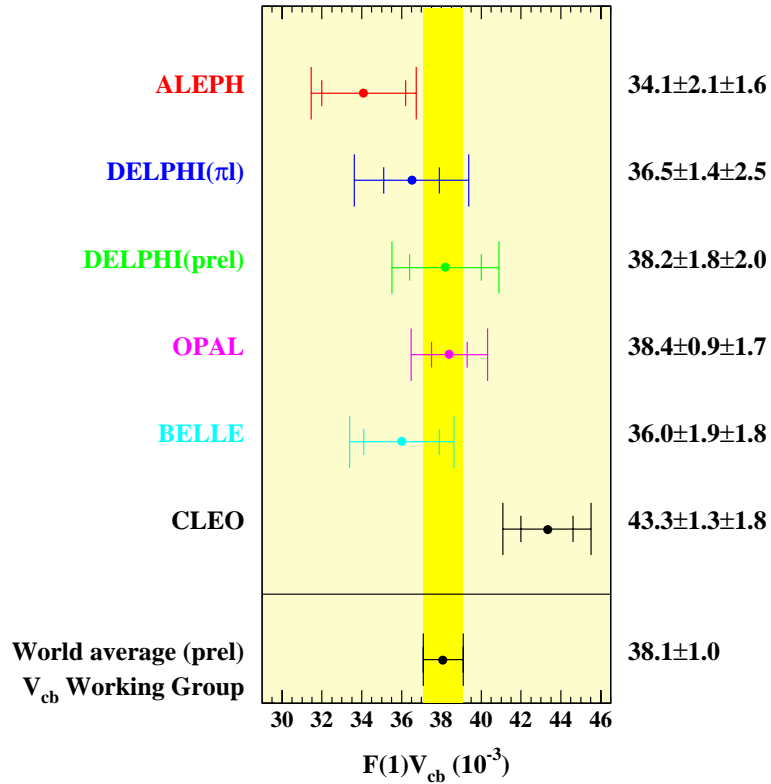
$$|V_{cb}| = (41.9 \pm 1.1 \pm 1.9(F(1)))10^{-3}(\text{exclusive}) \quad (5)$$

Combining the two determinations of  $|V_{cb}|$  (a possible correlation between the two determinations has been neglected) it gives<sup>2</sup>:

$$|V_{cb}| = (40.9 \pm 0.8)10^{-3}(\text{exclusive} + \text{inclusive}) \quad (6)$$

## 6 Measurement of $|V_{ub}|$ .

The CKM matrix element  $|V_{ub}|$  has been measured at LEP using semileptonic  $b$  to  $u$  decays. This measurement is rather difficult because one has to suppress the large background from the more abundant semileptonic  $b$  to  $c$  quark transitions. By using kinematical and topological variables, the LEP experiments have succeeded in measuring the semileptonic  $b$  to  $u$  branching ratio,<sup>7</sup> and obtain :


 Figure 7: Summary of the measurements of  $F(1) \times |V_{cb}|$ .<sup>5</sup>

$$BR(b \rightarrow l^- \bar{\nu} X_u) = (1.71 \pm 0.53) 10^{-3}$$

Using models based on the Operator Product Expansion, a value for  $|V_{ub}|$  is obtained :

$$|V_{ub}| = (40.9 \pm 6.1 \pm 3.1) \times 10^{-4} \quad \text{LEP} . \quad (7)$$

Prior to this analysis, the  $V_{ub}$  matrix element was firstly obtained, by CLEO and ARGUS collaborations, by looking at the spectrum of the lepton in B semileptonic decays. The difference between D meson and  $\pi$  masses is reflected in the momentum of the lepton from the B decays. This analysis have been recently revised by the CLEO Coll.. An alternative method to determine  $|V_{ub}|$  consists in the reconstruction of the charmless semileptonic B decays:  $B \rightarrow \pi(\rho)l\nu$ . This analysis has been performed by the CLEO Coll. and now by the b-factories. Figure 6 shows the full set of results on  $V_{ub}$ .<sup>8</sup>

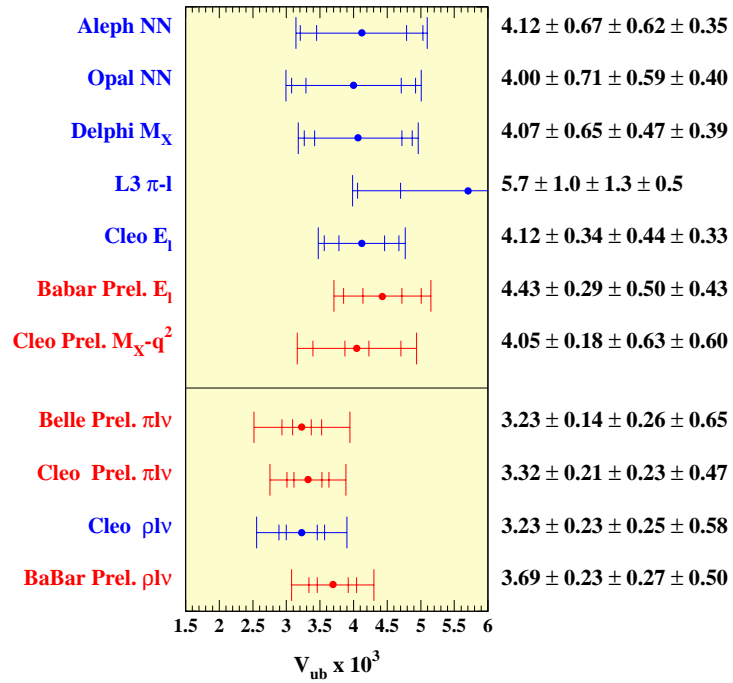


Figure 8: Summary of  $|V_{ub}|$  measurements.<sup>8</sup>

## 7 Study of $B^0 - \bar{B}^0$ oscillations

The probability that a  $B^0$  meson oscillates into a  $\bar{B}^0$  or remains a  $B^0$  is given by:

$$P_{B_q^0 \rightarrow B_q^0(\bar{B}_q^0)} = \frac{1}{2} e^{-t/\tau_q} (1 \pm \cos \Delta m_q t) \quad (8)$$

Where  $t$  is the proper time,  $\tau_q$  the lifetime of the  $B_q^0$  meson, and  $\Delta m_q = m_{B_1^0} - m_{B_2^0}$  the mass difference between the two physical mass eigenstates <sup>¶</sup>. To derive this formula the effects of CP violation and lifetime differences for the two states have been neglected.

Integrating expression 8, over the decay time, the probability to observe a  $\bar{B}_{d(s)}^0$  meson starting from a  $B_{d(s)}^0$  meson is given by  $\chi_d(s) = x_{d(s)}^2 / (2 + x_{d(s)}^2)$ , where  $x_{d(s)} = \Delta m_{d(s)} \tau(B_{d(s)}^0)$ . At Z energies, both  $B_d^0$  and  $B_s^0$  mesons are produced with fractions  $f_{B_d}$  and  $f_{B_s}$ . The average mixing parameter  $\chi$  is defined as :  $\chi = f_{B_d} \chi_d + f_{B_s} \chi_s$ . It has to be noted that for fast  $B_s^0$  oscillations  $\chi_s$  takes values close to 0.5 and  $\chi_s$  becomes very insensitive to  $x_s$ . Even a very precise measurement of  $\chi_s$  does not allow a determination of  $\Delta m_s$ .

It is then clear that only the time evolution of the  $B^0 - \bar{B}^0$  oscillations allow to measure  $\Delta m_d$  and  $\Delta m_s$ .

A time dependent study of  $B^0 - \bar{B}^0$  oscillations requires:

- the measurement of the proper time  $t$ ,
- to know if a  $B^0$  or a  $\bar{B}^0$  decays at time  $t$  (decay tag)
- to know if a  $b$  or a  $\bar{b}$  quark has been produced at  $t = 0$  (production tag).

In the Standard Model,  $B^0 - \bar{B}^0$  oscillations occur through a second-order process - a box diagram - with a loop of W and up-type quarks. The box diagram with the exchange of a *top* quark gives the dominant contribution :

$$\begin{aligned} \Delta m_d &\propto V_{td}^2 f_{B_d}^2 B_{B_d} \propto V_{cb}^2 \lambda^2 [(1 - \bar{\rho})^2 + \bar{\eta}^2] f_{B_d}^2 B_{B_d} \\ \Delta m_s &\propto V_{ts}^2 f_{B_s}^2 B_{B_s} \propto V_{cb}^2 f_{B_s}^2 B_{B_s} \\ \frac{\Delta m_d}{\Delta m_s} &\propto 1/\xi^2 | \frac{V_{td}}{V_{ts}} |^2 \propto 1/\xi^2 \lambda^2 [(1 - \bar{\rho})^2 + \bar{\eta}^2] \end{aligned} \quad (9)$$

$$\text{where } \xi = \frac{f_{B_s} \sqrt{B_{B_s}}}{f_{B_d} \sqrt{B_{B_d}}} .$$

Thus, the measurement of  $\Delta m_d$  and  $\Delta m_s$  gives access to the CKM matrix elements  $|V_{td}|$  and  $|V_{ts}|$  respectively. The difference in the  $\lambda$  dependence of these

<sup>¶</sup> $\Delta m_q$  is usually given in  $\text{ps}^{-1}$ :  $1 \text{ ps}^{-1}$  corresponds to  $6.58 \cdot 10^{-4} \text{ eV}$ .

expressions ( $\lambda \sim 0.22$ ) implies that  $\Delta m_s \sim 20 \Delta m_d$ . It is then clear that a very good proper time resolution is needed to measure the  $\Delta m_s$  parameter. On the other hand the measurement of the ratio  $\Delta m_d/\Delta m_s$  gives the same constraint as  $\Delta m_d$  but this ratio is expected to have smaller theoretical uncertainties since the ratio  $\xi$  is better known than the absolute value of  $f_B\sqrt{B_B}$ .

### $\Delta m_d$ measurements

Analyses using different events sample have been performed at LEP. A typical time distribution is shown in Figure 9.  $B_d^0 - \bar{B}_d^0$  oscillations with a frequency  $\Delta m_d$  are clearly visible. This can be a textbook plot ! The present summary of these results on  $\Delta m_d$ , is shown in Figure 10. Combining LEP, CDF and SLD measurements it follows that<sup>9</sup>:

$$\Delta m_d = (0.498 \pm 0.013) \text{ ps}^{-1} \quad (10)$$

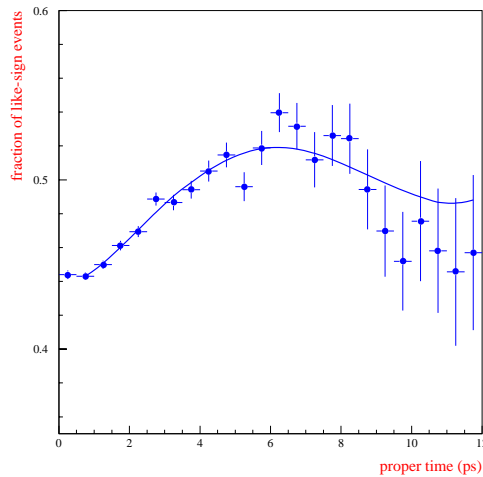


Figure 9: *This plot shows the fraction of like-sign events as a function of the proper decay time. Points with error bars are the data. The curve corresponds to the result of the fit to  $\Delta m_d$ .*

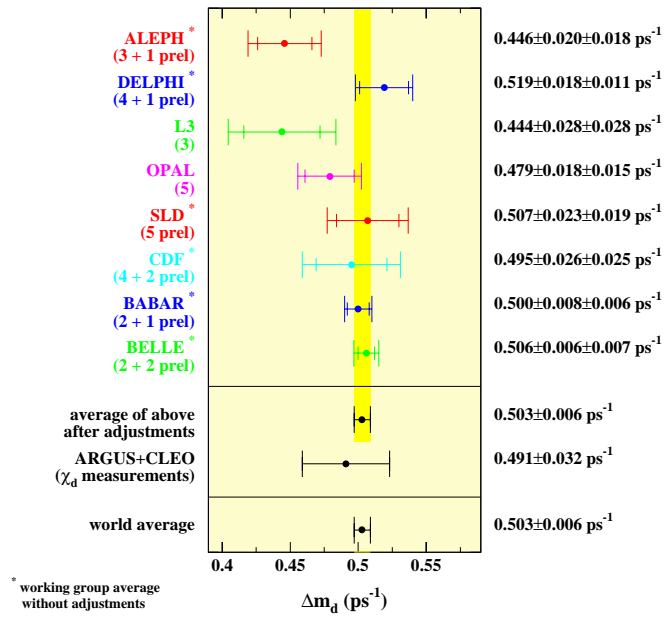


Figure 10: Summary of the  $\Delta m_d$  results from LEP, SLD, CDF, BABAR and BELLE.

$\Delta m_d$  has been first measured with high precision by the LEP/SLD/CDF experiments. The new and precise measurements performed at the B-Factories confirmed these measurements and improved the precision by a factor two. The combined result is now :  $\Delta m_d = (0.503 \pm 0.006) ps^{-1}$ . The evolution, over the years, of the combined  $\Delta m_d$  frequency measurement is shown in Figure 11.

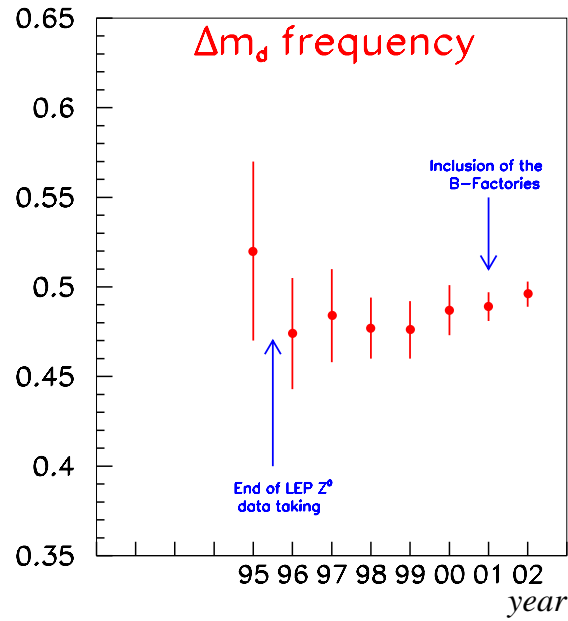


Figure 11: *The evolution of the combined  $\Delta m_d$  frequency measurement over the years.*

## Analyses on $\Delta m_s$

The search for  $B_s^0 - \overline{B}_s^0$  oscillations is more difficult because the oscillation frequency is much higher. In the Standard Model one expects  $\Delta m_s \sim 20 \Delta m_d$ . The proper time resolution will therefore play an essential role. Five different types of analyses have been performed at LEP/SLD. An overview is given in Table 2.

Analysis	N(events)	$P(B_S)$	$\varepsilon_1$	$\varepsilon_2$	$\sigma_t(t < 1\text{ps})$
Dipole	$\sim 700000$	$\sim 10\%$	$\sim 70\%$	$\sim 60\%$	$\sim 0.25$ ps
Inclusive lepton	$\sim 50000$	$\sim 10\%$	$\sim 70\%$	$\sim 90\%$	$\sim 0.25$ ps
$D_s^\pm h^\mp$	$\sim 3000$	$\sim 15\%$	$\sim 72\%$	$\sim 90\%$	$\sim 0.22$ ps
$D_s^\pm \ell^\mp$	$\sim 400$	$\sim 60\%$	$\sim 78\%$	$\sim 90\%$	$\sim 0.18$ ps
Exclusive $B_S^0$	$\sim 25$	$\sim 70\%$	$\sim 78\%$	$\sim 100\%$	$\sim 0.08$ ps

Table 2: Characteristics of the different analyses are given in terms of statistics ( $N$ ),  $B_s^0$  purity [ $P(B_S)$ ], tagging purities - i.e. the fraction of correctly tagged events - at the production and decay time ( $\varepsilon_1, \varepsilon_2$ ) and average time resolution within the first picosecond.

The so-called amplitude method<sup>10</sup> has been developed to combine data from different experiments. It corresponds to the following change in equation 8:

$$1 \pm \cos \Delta m_s t \rightarrow 1 \pm A \cos \Delta m_s t$$

$A$  and  $\sigma_A$  are measured at fixed values of  $\Delta m_s$ . In case of a clear oscillation signal, the measured amplitude is compatible with  $A = 1$  at the corresponding value of  $\Delta m_s$ . With this method it is also easy to set an exclusion limit. The values of  $\Delta m_s$  excluded at 95% C.L. are those satisfying the condition  $A(\Delta m_s) + 1.645 \sigma_A(\Delta m_s) < 1$ . Furthermore, the sensitivity of the experiment can be defined as the value of  $\Delta m_s$  corresponding to  $1.645 \sigma_A(\Delta m_s) = 1$  (for  $A(\Delta m_s) = 0$ , namely supposing that the “true” value of  $\Delta m_s$  is well above the measurable value of  $\Delta m_s$ ).

During the last seven years impressive improvements in the analysis techniques allowed to improve the sensitivity of this search, as it can be seen in Figure 12. The combined result of the LEP/SLD/CDF<sup>9</sup> analyses, displayed as an amplitude vs  $\Delta m_s$  plot, is shown in Figure 13 and is:

$$\Delta m_s > 14.4 \text{ ps}^{-1} \text{ at } 95\% \text{ C.L.}$$

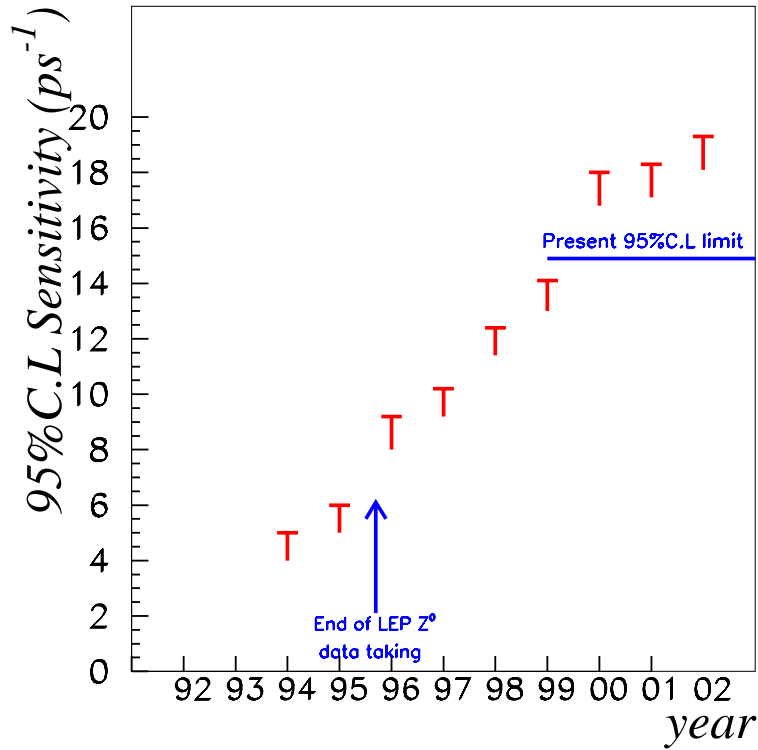


Figure 12: *The evolution, over the years, of the combined  $\Delta m_s$  sensitivity.*

The sensitivity is at  $19.2 \text{ ps}^{-1}$ .

The summary of the present results on  $\Delta m_s$  is shown in Figure 14.

The present combined limit implies that  $B_s^0$  oscillate at least 30 times faster than  $B_d^0$  mesons.

The significance of the “signal”, appearing around  $17 \text{ ps}^{-1}$ , is about  $2.5 \sigma$  and no claim can be made on the observation of  $B_s^0 - \bar{B}_s^0$  oscillations.

Tevatron experiments, are thus expected to measure soon  $B_s^0 - \bar{B}_s^0$  oscillations...

## 8 The CKM Matrix

In the Standard Model, the weak interactions among quarks are encoded in a  $3 \times 3$  unitary matrix: the CKM matrix. The existence of this matrix conveys the fact that quarks weak interaction eigenstates are a linear combination of their mass

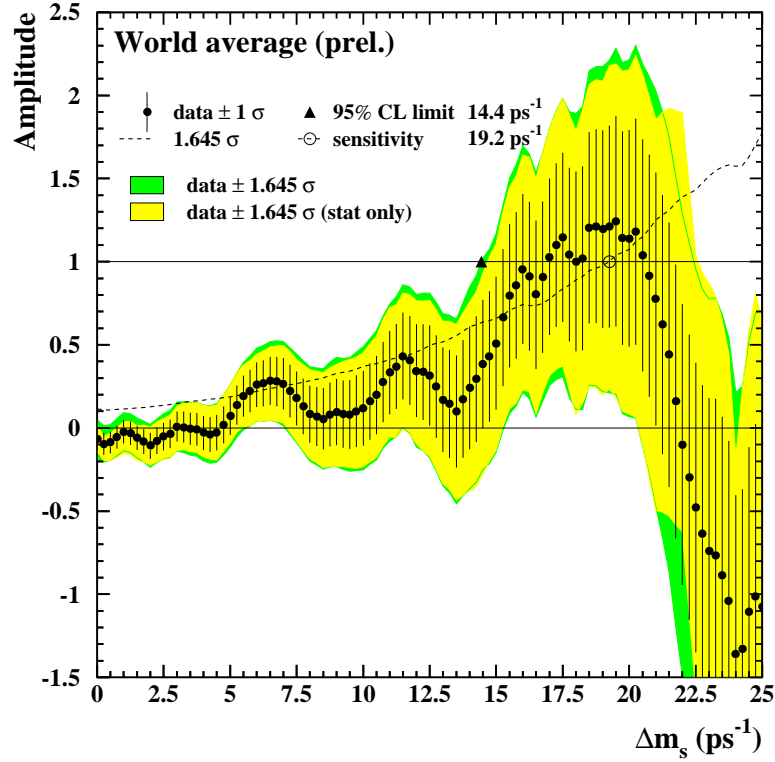


Figure 13: The plot shows the combined  $\Delta m_s$  results from LEP/SLD/CDF analyses displayed as an amplitude versus  $\Delta m_s$  plot. Points with error bars are the data; the lines show the 95% C.L. curves (darker regions include systematics).<sup>9</sup> The dotted curve shows the sensitivity.

eigenstates.<sup>11,12</sup>

$$V_{CKM} = \begin{pmatrix} V_{ud} & V_{us} & V_{ub} \\ V_{cd} & V_{cs} & V_{cb} \\ V_{td} & V_{ts} & V_{tb} \end{pmatrix} \quad (11)$$

The CKM matrix can be parametrized in terms of four free parameters. Here, the improved Wolfenstein<sup>13</sup> parametrization, expressed in terms of the four parameters  $\lambda$ ,  $A$ ,  $\rho$  and  $\eta$  (which accounts for the CP violating phase), will be used:

$$V_{CKM} = \begin{pmatrix} 1 - \frac{\lambda^2}{2} - \frac{\lambda^4}{8} & \lambda & A\lambda^3(\rho - i\eta) \\ -\lambda + \frac{A^2\lambda^5}{2}(1 - 2\rho) - iA^2\lambda^5\eta & 1 - \frac{\lambda^2}{2} - \lambda^4\left(\frac{1}{8} + \frac{A^2}{2}\right) & A\lambda^2 \\ A\lambda^3[1 - (1 - \frac{\lambda^2}{2})(\rho + i\eta)] & -A\lambda^2(1 - \frac{\lambda^2}{2})(1 + \lambda^2(\rho + i\eta)) & 1 - \frac{A^2\lambda^4}{2} \end{pmatrix} + O(\lambda^6). \quad (12)$$

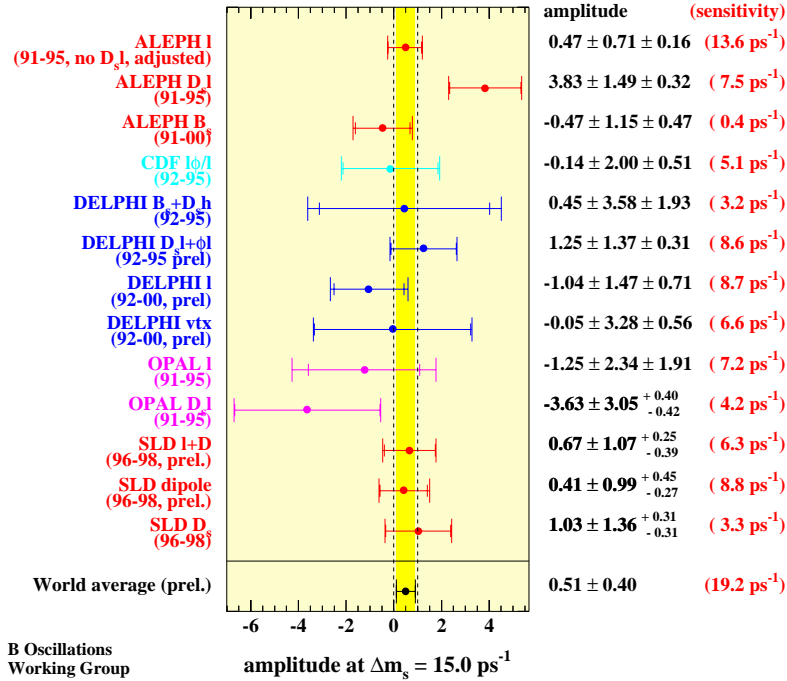


Figure 14: This plot shows the summary of results on the  $\Delta m_s$ , per experiment. Errors are given at  $\Delta m_s = 15 \text{ ps}^{-1}$  (the sensitivity is also indicated).

The CKM matrix elements can be expressed as:

$$V_{us} = \lambda V_{cb} = A\lambda^2, V_{ub} = A\lambda^3(\bar{\rho} - i\bar{\eta})/(1 - \lambda^2/2), V_{td} = A\lambda^3(1 - \bar{\rho} + i\bar{\eta}) \quad (13)$$

where the parameters  $\bar{\rho}$  and  $\bar{\eta}$  have been introduced<sup>14</sup> ||.

The parameter  $\lambda$  is precisely determined to be  $0.2210 \pm 0.0020$  \*\* using semileptonic kaon decays. The other parameters:  $A$ ,  $\bar{\rho}$  and  $\bar{\eta}$  were rather unprecisely known.

The Standard Model predicts relations between the different processes which depend upon these parameters; CP violation is accommodated in the CKM matrix and its existence is related to  $\bar{\eta} \neq 0$ . The unitarity of the CKM matrix can be vi-

$$\overline{\bar{\rho} = \rho(1 - \frac{\lambda^2}{2})} \quad ; \quad \overline{\bar{\eta} = \eta(1 - \frac{\lambda^2}{2})}.$$

\*\*due to the disagreement between the different determinations  $\lambda$  has been recently evaluated to be<sup>7</sup>:  $0.2237 \pm 0.0033$

sualized as a triangle in the  $\bar{\rho} - \bar{\eta}$  plane. Several quantities, depending upon  $\bar{\rho}$  and  $\bar{\eta}$  can be measured and they must define compatible values for the two parameters, if the Standard Model is the correct description of these phenomena. Extensions of the Standard Model can provide different predictions for the position of the upper vertex of the triangle, given by the  $\bar{\rho}$  and  $\bar{\eta}$  coordinates.

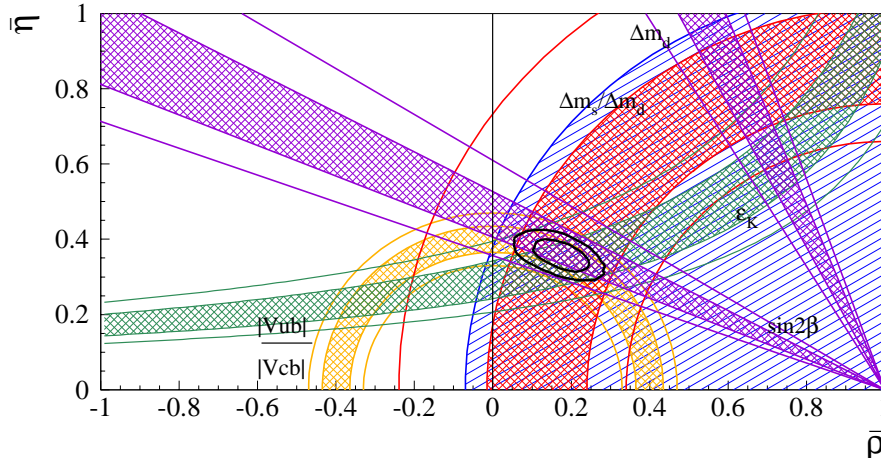


Figure 15: The allowed regions for  $\bar{\rho}$  and  $\bar{\eta}$  (contours at 68%, 95%) are compared with the uncertainty bands for  $|V_{ub}|/|V_{cb}|$ ,  $\epsilon_K$ ,  $\Delta m_d$ , the limit on  $\Delta m_s/\Delta m_d$  and  $\sin 2\beta$ .

Different constraints can be used to select the allowed region for the apex of the triangle in the  $\bar{\rho}-\bar{\eta}$  plane. Five have been used sofar:  $\epsilon_k$ ,  $|V_{ub}|/|V_{cb}|$ ,  $\Delta m_d$ , the limit on  $\Delta m_s$  and  $\sin 2\beta$  from the measurement of the CP asymmetry in  $J/\psi K^0$  decays. These constraints are shown in Figure 15.<sup>15</sup> These measurements provide a set of constraints which are obtained by comparing measured and expected values of the corresponding quantities, in the framework of the Standard Model (or of any other given model). In practice, theoretical expressions for these constraints involve several additional parameters such as quark masses, decay constants of B mesons and bag-factors. The values of these parameters are constrained by other measurements (e.g. the top quark mass) or using theoretical expectations. Different statistical methods have been defined to treat experimental and theoretical errors. The methods essentially differ in the treatment of the latter and can be classified into two main groups: frequentist and Bayesian. The net result is that, if the same inputs are used, the different statistical methods select quite

Parameter	Value	Gaussian $\sigma$	Uniform half-width	Ref.
$\lambda$	0.2210	0.0020	-	7
$ V_{cb} (\text{excl.})$	$42.1 \times 10^{-3}$	$2.1 \times 10^{-3}$	-	16
$ V_{cb} (\text{incl.})$	$40.4 \times 10^{-3}$	$0.7 \times 10^{-3}$	$0.8 \times 10^{-3}$	16
$ V_{ub} (\text{excl.})$	$32.5 \times 10^{-4}$	$2.9 \times 10^{-4}$	$5.5 \times 10^{-4}$	7
$ V_{ub} (\text{incl.})$	$40.9 \times 10^{-4}$	$4.6 \times 10^{-4}$	$3.6 \times 10^{-4}$	7
$\Delta m_d$	0.503 ps <sup>-1</sup>	0.006 ps <sup>-1</sup>	-	9
$\Delta m_s$	> 14.4 ps <sup>-1</sup> at 95% C.L.	sensitivity	19.2 ps <sup>-1</sup>	9
$m_t$	167 GeV	5 GeV	-	17
$f_{B_d} \sqrt{\hat{B}_{B_d}}$	235 MeV	33 MeV	${}^{+0}_{-24}$ MeV	18
$\xi = \frac{f_{B_s} \sqrt{\hat{B}_{B_s}}}{f_{B_d} \sqrt{\hat{B}_{B_d}}}$	1.18	0.04	${}^{+0.12}_{-0.00}$	18
$\hat{B}_K$	0.86	0.06	0.14	18
$\sin 2\beta$	0.734	0.054	-	19

Table 3: Values of the relevant quantities used in the fit of the CKM parameters. In the third and fourth columns the Gaussian and the flat parts of the uncertainty are given, respectively.<sup>20</sup> The values and the errors on  $V_{cb}$  are taken from<sup>16</sup> and are slightly different with respect to those given in equations 3,5.

similar values for the different CKM parameters.<sup>21</sup> The results in the following are shown using the Bayesian approach.

Central values and uncertainties taken for the relevant parameters used in these analyses are given in Table 3.<sup>20</sup>

The most crucial test is the comparison between the region selected by the measurements which are sensitive only to the sides of the Unitarity Triangle and the regions selected by the direct measurements of the CP violation in the kaon ( $\epsilon_K$ ) or in the B ( $\sin 2\beta$ ) sector. This test is shown in Figure 16.

It can be translated quantitatively in the comparison between the value of  $\sin 2\beta$  obtained from the measurement of the CP asymmetry in  $J/\psi K^0$  decays and the one determined from triangle “sides“ measurements,<sup>220</sup>:

$$\begin{aligned}
 \sin 2\beta &= 0.725^{+0.055}_{-0.065} && \text{triangle sides only} \\
 \sin 2\beta &= 0.734 \pm 0.054 && B^0 \rightarrow J/\psi K^0.
 \end{aligned}
 \tag{14}$$

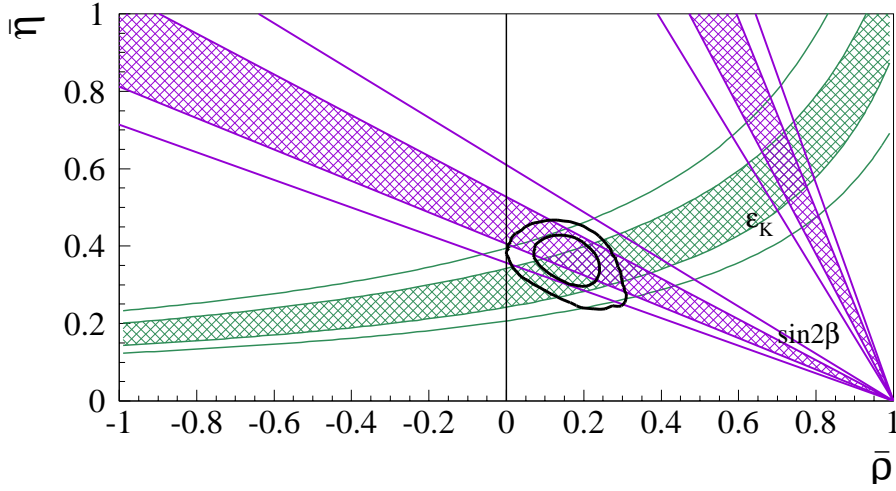


Figure 16: The allowed regions for  $\bar{\rho}$  and  $\bar{\eta}$  (contours at 68%, 95%) as selected by the measurement of  $|V_{ub}|/|V_{cb}|$ ,  $\Delta m_d$ , the limit on  $\Delta m_s/\Delta m_d$  are compared with the bands (at 1 and  $2\sigma$ ) selected from CP violation in the kaon ( $\epsilon_K$ ) and in the B ( $\sin 2\beta$ ) sectors.

The spectacular agreement between these values shows the consistency of the Standard Model in describing the CP violation phenomena in terms of one single parameter  $\eta$ . It is also an important test of the OPE, HQET and LQCD theories which have been used to extract the CKM parameters.

Including all five constraints the results are,<sup>220</sup>:

$$\begin{aligned}
 \bar{\eta} &= 0.357 \pm 0.027 & (0.305 - 0.411) \\
 \bar{\rho} &= 0.173 \pm 0.046 & (0.076 - 0.260) \\
 \sin 2\beta &= 0.725^{+0.035}_{-0.031} & (0.660 - 0.789) \\
 \sin 2\alpha &= -0.09 \pm 0.25 & (-0.54 - 0.40) \\
 \gamma &= (63.5 \pm 7.0)^\circ & (51.0 - 79.0)^\circ \\
 \Delta m_s &= (18.0^{+1.7}_{-1.5})ps^{-1} & (15.4 - 21.7)ps^{-1}.
 \end{aligned} \tag{15}$$

The ranges within parentheses correspond to 95% probability. The results on  $\Delta m_s$  and  $\gamma$  are predictions for those quantities which will be measured in near future.

## 9 Conclusions

During the last ten years, our understanding of the flavour sector of the Standard Model improved. LEP and SLD played a central role.

At the start of LEP and SLD, only the  $B_d$  and the  $B^+$  hadrons were known and their properties were under study. Today B hadrons have been carefully studied and many quantities have already been measured with good precision. The hadron lifetimes are now measured at the one/few percent level. LEP experiments are the main contributors for the measurement of  $|V_{cb}|$ , which is known with a relative precision better than 2%. In this case, not only, the decay width has been measured, but also some of the non-perturbative QCD parameters entering in its expression. It is a great experimental achievement and a success for the theory description of the non-perturbative QCD phenomena in the framework of the OPE. LEP experiments have been pioneering in determining  $|V_{ub}|$  using inclusive methods and reaching a precision of about 10%, defining a road for future measurements at B-factories.

The time behaviour of  $B^0 - \bar{B}^0$  oscillations has been studied and precisely measured in the  $B_d^0$  sector. The new and precise measurements performed at the B-Factories confirmed these measurements and improved the precision by a factor two. The oscillation frequency  $\Delta m_d$  is known with a precision of about 1%.  $B_s^0 - \bar{B}_s^0$  oscillations have not been measured so far, but this search has pushed the experimental limit on the oscillation frequency  $\Delta m_s$  well beyond any initial prediction for experimental capabilities. SLD experiment have played a central role in this search. Today we know that  $B_s^0$  oscillate at least 30 times faster than  $B_d^0$  mesons. The frequency of the  $B_s^0 - \bar{B}_s^0$  oscillations will be soon measured at the Tevatron. Nevertheless the impact of the actual limit on  $\Delta m_s$  for the determination of the unitarity triangle parameters is crucial.

The unitarity triangle parameters are today known within good precision. The evolution of our knowledge concerning the allowed region in the  $\bar{\rho}-\bar{\eta}$  plane is shown in Figure 17. The reduction in size of the error bands, from the year 1995 to 2000, is essentially due to the analyses described in this paper and to the progress in the OPE, HQET and LQCD theories. The reduction between 2000 and 2002 is also driven by the precise measurements of  $\sin 2\beta$  at the  $b$ -factories.

A crucial test has been already done: the comparison between the unitarity triangle parameters, as determined with quantities sensitive to the sides of the unitarity

triangle (semileptonic B decays and oscillations), with the measurements of CP violation in the kaon ( $\epsilon_K$ ) and in the B ( $\sin 2\beta$ ) sectors. This agreement tells us that the Standard Model is also working in the flavour sector and it is also an important test of the OPE, HQET and LQCD theories which have been used to extract the CKM parameters. On the other hand, these tests are at about 10% level accuracy, the current and the next facilities can surely push these tests to a 1% level.

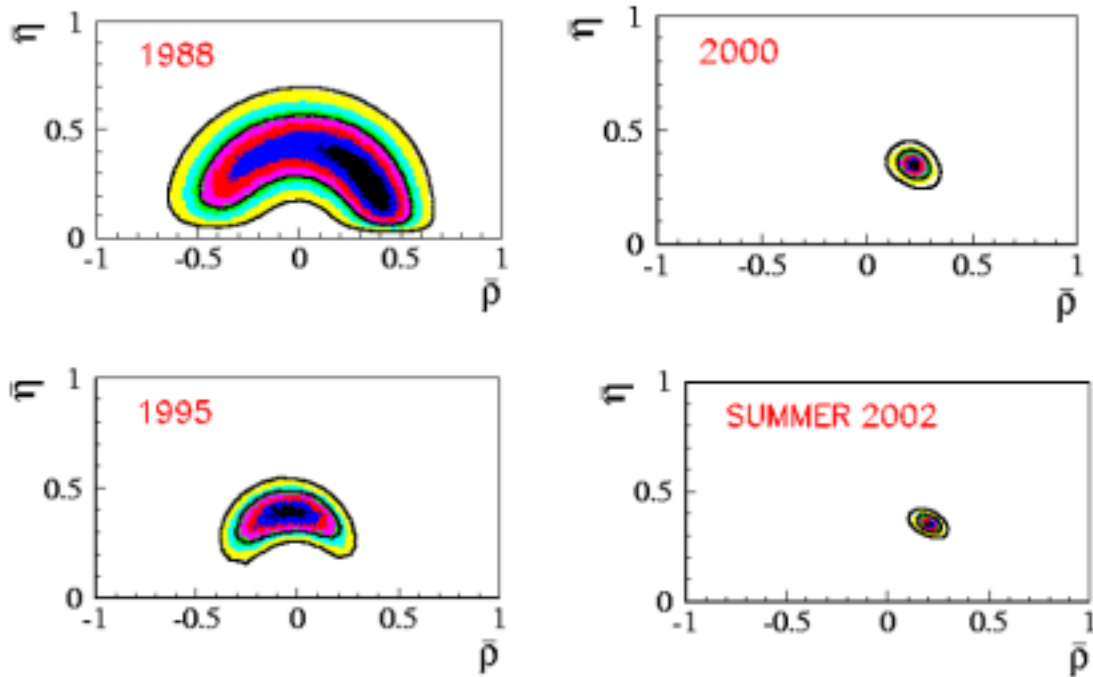


Figure 17: *Evolution, over the years, of the allowed regions for  $\bar{\rho}$  and  $\bar{\eta}$  (contours at 68%, 95%).*

## 10 Acknowledgements

I would like to thank the organisers for the invitation and for having set up a very interesting topical conference in a stimulating and nice atmosphere during and after the talks.

Thanks to all the LEP and SLD members which have made all of it possible! I

would also like to remember the important work made from the members of the Heavy Flavour Working Groups who prepared a large fraction of the averages quoted in this note. They are all warmly thanked.

Thanks to P. Roudeau for the careful reading of the manuscript.

## References

- [1] ALEPH, CDF, DELPHI, L3, OPAL, SLD Collaborations, CERN-EP/2001-050
- [2] A. Stocchi, plenary talk given at the XXXI<sup>th</sup> ICHEP, Amsterdam 24-31 July 2002, hep-ph/0211245.
- [3] LEP B Lifetime Working Group:  
<http://lepbose.web.cern.ch/LEPBOSC/lifetimes/lepblife.html>
- [4] E.Franco, V.Lubicz, F. Mescia, C.Tarantino, Nucl.Phys. B633 (2002) 212. (hep-ph/02030890).
- [5]  $V_{cb}$  Working Group: <http://lepvcb.web.cern.ch/LEPVCB/>
- [6] L. Lellouch, plenary talk given at the XXXI<sup>th</sup> ICHEP, Amsterdam 24-31 July 2002 ; A. S. Kronfeld, P. B. Mackenzie, J. N. Simone, S. Hashimoto, S. M. Ryan, proceedings of FPCP, May 16–18, Philadelphia, Pennsylvania (hep-ph/0110253); Phys.Rev. D66 (2002) 014503.
- [7] Results presented at the CKM Unitarity Triangle Workshop, CERN Feb 2002:  
<http://ckm-workshop.web.cern.ch/ckm-workshop/> in particular see also:  
LEP Working group on  $|V_{cb}|$ : <http://lepvcb.web.cern.ch/LEPVCB/> Winter 2002 averages.  
LEP Working group on  $|V_{ub}|$ :  
<http://battagl.home.cern.ch/battagl/vub/vub.html>.
- [8] M. Battaglia, talk given at the XXXI<sup>th</sup> ICHEP, Amsterdam 24-31 July 2002.
- [9] LEP Working group on oscillations:  
[http://lepbose.web.cern.ch/LEPBOSC/combined\\_results/amsterdam\\_2002/](http://lepbose.web.cern.ch/LEPBOSC/combined_results/amsterdam_2002/).
- [10] H.G. Moser and .A. Roussarie, Nucl. Instum. Meth. A384 (1997) 491.

- [11] N. Cabibbo, Phys. Rev. Lett. 10 (1963) 531.
- [12] M. Kobayashi and K. Maskawa, Prog. Theor. Phys. 49 (1973) 652.
- [13] L. Wolfenstein, Phys. Rev. Lett. **51** (1983) 1945.
- [14] A.J. Buras, M.E. Lautenbacher and G. Ostermaier, Phys.Rev. **D50** (1994) 3433.
- [15] For details see : M. Ciuchini et al., JHEP 0107:013, 2001 hep-ph/0012308.
- [16] M. Artuso and E. Barberio, hep-ph/0205163.
- [17] F. Abe *et al.*, CDF Collaboration, Phys. Rev. Lett. **74** (1995) 2626.  
S. Abachi *et al.*, D0 Collaboration, Phys. Rev. Lett. **74** (1995) 2632.
- [18] L. Lellouch, plenary talk given at the XXXI<sup>th</sup> ICHEP, Amsterdam 24-31 July 2002.
- [19] Average from Y. Nir see these proceedings based on: R. Barate et al. (ALEPH Collaboration) *Phys. Lett.* **B492** (2000), 259-274; K. Ackerstaff et al. (OPAL Collaboration) *Eur. Phys. J.* **C5** (1998) 379; T. Affolder et al. Phys. Rev. D61 (2000) 072005; B. Aubert et al. (Babar Collaboration) hep-ex/0207042; K. Abe et al. (Belle Collaboration) hep-ex/0207098.
- [20] F. Parodi, talk given at the XXXI<sup>th</sup> ICHEP, Amsterdam 24-31 July 2002.
- [21] Results presented at the CKM Unitarity Triangle Workshop, CERN Feb 2002. <http://ckm-workshop.web.cern.ch/ckm-workshop/>  
For the description of the methods see:  
M. Ciuchini *et al.*, JHEP **0107** (2001) 013 (hep-ph/0012308).  
A. Höcker, H. Lacker, S. Laplace, F. Le Diberder, *Eur. Phys. J.* **C21**, 225 (2001).  
G. P. Dubois-Felsmann D. G. Hitlin, F. C. Porter and G. Eigen, CALT 68-2396 June2002.